Numerical treatment and optimal control of the hepatitis B virus spatio-temporal model

Khalid K. Ali[1,2,*]**, Kamal R. Raslan**[2]**, Ahmed F. Koura**[3]**, and Mohamed Abozeid Shaalan**[4]

[1]Mathematics Education Program, Faculty of Education and Arts, Sohar University, Sohar 311, Oman.

[2]Mathematics Department, Faculty of Science, Al-Azhar University, Nasr-City, Cairo, Egypt.

[3]Basic Science Department, Al-Safwa High Institute of Engineering, Egypt.

[4]Higher Technological Institute, Tenth of Ramadan City, Egypt.

Abstract

In this article, we propose an optimal control of the hepatitis B virus (HBV) infection model. We use four control functions in this model to show the effect of quarantine, vaccination, treatment, and rapid testing in minimizing the infection between individuals. We apply Pontryagin's maximum principle to study these four controls. We solve the mathematical model without control and after adding control functions using by finite difference scheme. We show the results graphically. In addition, we study the HBV spatio-temporal model numerically and discuss the truncation error and the stability of its numerical scheme.

---

1. INTRODUCTION

In the last few years, mathematical modeling has been widely used to investigate the transmission and dynamics of infectious diseases. Hepatitis B is a contagious disease caused by HBV that primarily affects the human liver and can causes cancer or failure of liver. Transmission of this disease has many causes, including food and drink, transfusion of contaminated blood, sexual relations, use of personal items of the infected person, and from the infected mother to the newborn child. Khan et al. [8] created a mathematical epidemiological model of hepatitis B disease. Ahmad et al. [1] investigated a fractional order model that describes the dynamics of hepatitis B. Zou et al. [17] established a mathematical model for understanding the dynamical transmission and the spread of hepatitis B virus infection in China, which provided an approximate estimate of the basic reproduction number. Sharomi and Malik [14] demonstrated that optimal control theory has proven to be a successful tool in understanding ways to prevent the spread of infectious diseases. Akbari and Asheghi [2] proposed an optimal control mathematical problem for an HIV infection model. Saha and Samanta [13] suggested a compartmental model for the transmission of HIV/AIDS, including treatment and Pre-exposure prophylaxis (PrEP). Zorom et al. [16] presented a treatment and prevention model for malaria with two different control variables. Gaff [7] suggested the most effective mitigation strategy to reduce the number of people infected by balancing treatment and vaccination, which applied to models with different cost scenarios. Raza et al. [12] studied the dynamical behavior of human-immune-efficiency-virus by investigating a nonlinear delayed model. Manna and Hattaf [10] established and analyzed a new mathematical differential equations model for understanding the dynamics of hepatitis B virus (HBV) infection. Bachraoui et al. [4] investigated a fractional diffusive model for hepatitis B virus infection. Subchan et al. [6] discussed the mathematical modeling of cholera disease spread. Zaman et al. [15] introduced a time delay control strategy to combat the SIR epidemic model. Alrabaiah et al. [3] established a mathematical control model to study the dynamical behavior of the hepatitis B virus.

---

* Corresponding author. Email: khalidkaram2012@yahoo.com.

Neilan et al. [11] formulated a mathematical model to include such basic components as a highly contagious and short-lived bacterial condition, a separate category for mild human infection, and diminished disease immunity. Koura et al. [9] introduced a numerical study of a spatio-temporal coronavirus pandemic. Anwarud et al. [5] established a control model in order to eliminate the hepatitis B virus from the population and demonstrated that the control model did exist.

This article is arranged as follows: In section 2, the mathematical model and numerical solution of the temporal model are presented. In section 3, the implementation of the optimal control problem and numerical simulation are given. The spatio-temporal model and its numerical solution, with the study of the truncation error and stability of this numerical scheme, are introduced in section 4. In section 5, the conclusion of the illustrated outcomes.

2. Mathematical model

The literature reveals that the different stages of hepatitis B, along with factors such as migration, hospitalization, and vaccination, significantly influence the spread and control of the disease. To the best of our knowledge, no mathematical model has yet been proposed that incorporates these various phases alongside the effects of treatment, migration, and vaccination. Developing such a model would provide a more comprehensive understanding of the dynamics of hepatitis B transmission and control. To formulate the hepatitis B virus model [8], we divide the population of humans into seven categories: susceptible people $S(t)$, people with inactive infection $I_l(t)$, people with mild infection $I(t)$, chronically infected people $I_c(t)$, hospitalized people $I_h(t)$, recovered people $R(t)$, and vaccinated individuals $V(t)$. The temporal model (2.1) consists of seven ordinary differential equations for the dynamic transmission of the hepatitis B virus:

$$
\begin{aligned}
\frac{dS}{dt} &= \Lambda_1\Lambda_2(1 - \alpha I_c(t)) + \theta V(t) - (\omega I(t) + \rho\omega I_c(t) + \gamma_3 + d_0 + \mu)S(t), \\
\frac{dI_l}{dt} &= (\omega I(t) + \rho\omega I_c(t))S(t) - (\eta_1 + d_0 + \mu)I_l(t), \\
\frac{dI}{dt} &= -(\beta_1 + \gamma_1 + d_0 + \mu)I(t) + \eta_1 I_l(t), \\
\frac{dI_c}{dt} &= \eta_3\gamma_1 I(t) - (\beta_2\eta_2 + d_0 + d_1 - \Lambda_1\Lambda_2\alpha)I_c(t), \\
\frac{dI_h}{dt} &= \beta_2 I_c(t) + \beta_1 I(t) - (\beta_3 + d_0 + d_2)I_h(t), \\
\frac{dR}{dt} &= \eta_2 I_c(t) + (1 - \eta_3)\gamma_1 I(t) + \beta_3 I_h(t) - d_0 R(t), \\
\frac{dV}{dt} &= \Lambda_1(1 - \Lambda_2) + \gamma_3 S(t) - (\theta + d_0)V(t),
\end{aligned}
\tag{2.1}
$$

with initial values $S(0)$, $I_l(0)$, $I(0)$, $I_c(0)$, $I_h(0)$, $R(0)$, and $V(0) \geq 0$.

In system (2.1), Λ_1 is the newborn rate, Λ_2 is the rate of newborns without vaccination, α is the proportion of the population with infections inherited from parents and θ is the rate of acquired immunity from vaccination after weaning. The parameters β_1, β_2, and β_3 describe the transmission rate from I class to I_h class, the transmission rate from I_c class to I_h class, and the recovery rate in I_h class, respectively. ω is the transfer degree, while ρ is the reduced transfer degree. The parameters η_1, η_2, and η_3 describe the transmission rate from I_l class to I class, transmission rate from I_c class to R class, and recovery failure rate in I class, respectively. d_0, d_1, and d_2 are the death rates in natural death, I_c class death, and I_h class death, respectively. μ is the peregrination rate.

2.1. **Region of stability.** In this subsection, we introduce some important indicators that help us explain the spread of the pandemic in the population. The number of new infections caused by an infectious individual in a disease-free population is defined as the reproduction number R_0. If $R_0 > 1$, the epidemic will spread, while it will be confined if $R_0 < 1$. Reproduction number R_0 for the temporal system (2.1) discussed in [8] is as follows:

$$
R_0 = \frac{\gamma_1 S_0 \eta_3 \eta_1 \rho\omega}{(d_0 + \eta_1 + \mu)(\beta_1 + \gamma_1 + d_0 + \mu)(-\alpha\Lambda_1\Lambda_2 + \beta_2\eta_2 + d_0 + d_1)} + \frac{S_0\eta_1\omega}{(d_0 + \eta_1 + \mu)(\beta_1 + \gamma_1 + d_0 + \mu)},
\tag{2.2}
$$

(a) $(\eta_1, \omega, \Lambda_2)$ space

(b) $\eta_1, \omega, \Lambda_2 = 1$

(c) $\eta_1, \omega, \Lambda_2 = 0.3$
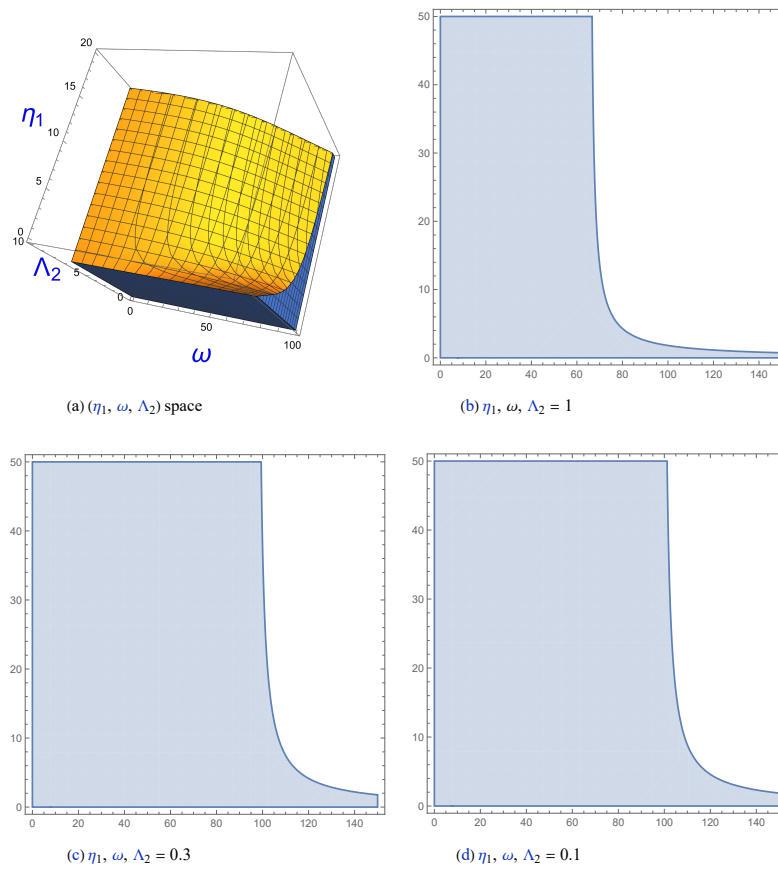
(d) $\eta_1, \omega, \Lambda_2 = 0.1$

FIGURE 1. Stability region for the disease-free equilibrium point.

where S_0 defined as

$$S_0 = \frac{\Lambda_1 (d_0 \Lambda_2 + \theta)}{d_0 (\gamma_3 + d_0 + \theta + \mu) + \theta \mu}. \tag{2.3}$$

The stability region of the disease-free equilibrium point shows $(\eta_1, \omega, \Lambda_2)$ space in Figure 1(a). The values of parameters are discussed in [8] as $\Lambda_1 = 0.0121$, $\alpha = 0.11$, $\theta = 0.1$, $\beta_1 = 0.36$, $\beta_2 = 0.59$, $\beta_3 = 0.311$, $\rho = 0.16$, $\eta_2 = 0.0000684$, $\eta_3 = 0.885$, $d_0 = 0.0069$, $d_1 = 0.002$, $d_2 = 0.002$, and $\mu = 0.95$.

In Figures 1(b, c, d), we find that the region of stability increases with a decrease in the value of Λ_2, so we can get a stable solution with small values of $(\eta_1, \omega, \Lambda_2)$. The values of η_1, ω, and Λ_2 are taken from the stability region study as 0.016, 0.95, and 0.32, respectively.

2.2. **Numerical solution of the temporal HBV model.** For the numerical solution of the temporal model (2.1), we apply the forward finite difference scheme as in the following steps:

Step 1: Discretize the domain by dividing the domain of $t \in [0, 50]$ with step size $\Delta t = 1$.

Step 2: Apply the forward finite difference method to approximate the derivatives in the differential equations. For each equation in the system (2.1), replace the derivatives with forward finite difference approximations:

$$\frac{\partial S}{\partial t} = \frac{(S)_j^{m+1} - (S)_j^m}{\Delta t}. \tag{2.4}$$

Step 3: Discretize the system of equations and convert it into a system of algebraic equations as follows:

$$(S)^{m+1} = (S)^m + \Delta t\theta(V)^m + \Delta t\Lambda_1\Lambda_2\Big(1 - \alpha(I_c)^m + 1\Big) - \Delta t\Big(\omega(I)^m + \rho\omega(I_c)^m + \gamma_3 + d_0 + \mu\Big)(S)^m, \quad (2.5)$$

$$(I_l)^{m+1} = (I_l)^m + \Delta t\Big(\omega(I)^m + \rho\omega(I_c)^m\Big)(S)^m - \Delta t\Big(\eta_1 + d_0 + \mu\Big)(I_l)^m, \tag{2.6}$$

$$(I)^{m+1} = (I)^m - \Delta t\Big(\beta_1 + \gamma_1 + d_0 + \mu\Big)(I)^m + \Delta t\eta_1(I_l)^m, \tag{2.7}$$

$$(I_c)^{m+1} = (I_c)^m + \Delta t\eta_3\gamma_1(I)^m - \Delta t\Big(\beta_2\eta_2 + d_0 + d_1 - \Lambda_1\Lambda_2\alpha\Big)(I_c)^m, \tag{2.8}$$

$$(I_h)^{m+1} = (I_h)^m - \Delta t\Big(\beta_3 + d_0 + d_2\Big)(I_h)^m + \Delta t\beta_2(I_c)^m + \Delta t\beta_1(I)^m, \tag{2.9}$$

$$(R)^{m+1} = (R)^m + \Delta t\eta_2(I_c)^m + \Delta t\Big(1 - \eta_3\Big)\gamma_1(I)^m + \Delta t\beta_3(I_h)^m - \Delta td_0(R)^m, \tag{2.10}$$

$$(V)^{m+1} = (V)^m + \Delta t\Lambda_1\Big(1 - \Lambda_2\Big) + \Delta t\gamma_3(S)^m - \Delta t\Big(\theta + d_0\Big)(V)^m. \tag{2.11}$$

Step 4: With the initial conditions $S(0) = 100$, $I_l(0) = 100$, $I(0) = 80$, $I_c(0) = 70$, $I_h(0) = 50$, $R(0) = 40$, and $V(0) = 40$. Update the values of the variables at each grid point based on the solution obtained.

Step 5: Repeat iteratively and use Mathematica 12 package to maintain numerical results for system (2.1) using the forward finite difference method as shown in Figure 2 with blue color.

3. Optimal control problem

In this section, we use optimal control theory for the HBV model (2.1). We apply four different controls to minimize the infection and spread of the HBV in the community. The first control u_i is the prevention or quarantine control, which reduces infection by minimizing contact between infected and healthy individuals. The second control u_v denotes the vaccination control to reduce infection. The third control u_r denotes a rapid test for people in the I_l category to identify infections and quarantine them. The fourth control u_t regards treatment control.

This discussion leads us to the following optimal control problem:

$$\frac{dS}{dt} = \Lambda_1\Lambda_2(1 - \alpha I_c(t)) + \theta V(t) - (\omega I(t) + \rho\omega I_c(t))(1 - u_i)S(t) - (\gamma_3 u_v + d_0 + \mu)S(t),$$

$$\frac{dI_l}{dt} = (\omega I(t) + \rho\omega I_c(t))(1 - u_i)S(t) - (\eta_1(1 - u_r) + d_0 + \mu)I_l(t),$$

$$\frac{dI}{dt} = -(\beta_1 u_t + \gamma_1 + d_0 + \mu)I(t) + \eta_1 u_r I_l(t),$$

$$\frac{dI_c}{dt} = \eta_3\gamma_1 I(t) - (\beta_2 u_t \eta_2 + d_0 + d_1 - \Lambda_1\Lambda_2\alpha)I_c(t), \tag{3.1}$$

$$\frac{dI_h}{dt} = \beta_2 u_t I_c(t) + \beta_1 u_t I(t) - (\beta_3 u_t + d_0 + d_2)I_h(t),$$

$$\frac{dR}{dt} = \eta_2 I_c(t) + (1 - \eta_3)\gamma_1 I(t) + \beta_3 u_t I_h(t) - d_0 R(t),$$

$$\frac{dV}{dt} = \Lambda_1(1 - \Lambda_2) + \gamma_3 u_v S(t) - (\theta + d_0)V(t).$$

Now, we define an objective function:

$$J(u_i(t), u_v(t), u_r(t), u_t(t)) = \int_0^t (k_1 I_l + k_2 I + k_3 I_c + k_4 I_h + 0.5k_5 u_i^2(t) + 0.5k_6 u_v^2(t) + 0.5k_7 u_r^2(t) + 0.5k_8 u_t^2(t))dt, \tag{3.2}$$

subject to the control system (3.1), t denotes the final time of the treatment and the parameters k_i with $i = 1, 2, ..., 7$ are the weight factors for the balancing constants. The quadratic expressions of $u_i(t), u_v(t), u_r(t)$, and $u_t(t)$ are nonlinear costs of intervention. The controls defined above are continuous Lebesgue integrable; we aim to minimize

the objective function (3.2) for minimizing HBV infection between people by finding optimal controls $u_i^*(t)$, $u_v^*(t)$, $u_r^*(t)$, and $u_t^*(t)$ such that:

$$J(u_i^*(t), u_v^*(t), u_r^*(t), u_t^*(t)) = min\{J(u_i(t), u_v(t), u_r(t), u_t(t)) \; : (u_i(t), u_v(t), u_r(t), u_t(t)) \in U\}, \tag{3.3}$$

where U denoted to be a measurable control set:

$$U = \{(u_i(t), u_v(t), u_r(t), u_t(t)) : [0, t] \to [0, 1]\}. \tag{3.4}$$

3.1. **characterization of optimal control.** The necessary conditions for the existence of optimal control should satisfy Pontryagin's maximum principle, which states that if $u_i^*(t), u_v^*(t), u_r^*(t), u_t^*(t) \in U$ are an optimal control for (3.2) with a fixed final time t, then there exists an adjoint vector with seven adjoint variables λ_i for $i = 0, 1, 2, ..., 7$ associated with the state variables S, I_l, I, I_c, I_h, V, and R. This principle converts the optimal control system (3.1) with the objective function (3.2) into a problem of minimizing a Hamiltonian H with the controls (u_i, u_v, u_r, u_t).

The Hamiltonian of this problem is defined as:

$$\begin{aligned} H = {}& k_1 I_l + k_2 I + k_3 I_c + k_4 I_h + 0.5 k_5 u_i^2(t) + 0.5 k_6 u_v^2(t) + 0.5 k_7 u_r^2(t) \\ & + 0.5 k_8 u_t^2(t) + \lambda_1 \frac{dS}{dt} + \lambda_2 \frac{dI_l}{dt} + \lambda_3 \frac{dI}{dt} + \lambda_4 \frac{dI_c}{dt} + \lambda_5 \frac{dI_h}{dt} + \lambda_6 \frac{dR}{dt} + \lambda_7 \frac{dV}{dt}. \end{aligned} \tag{3.5}$$

Theorem 3.1. *There exist adjoint variables $\lambda_i(t)$, $i = 1, 2, 3, ..., 7$, associated with the state variables S, I_l, I, I_c, I_h, V, and R such that the optimal controls $u_i^*(t), u_v^*(t), u_r^*(t), u_t^*(t)$ and the solution $S^*, I_l^*, I^*, I_c^*, I_h^*, V^*$ satisfy universality conditions. Furthermore, we have the controls:*

$$u_i^* = min\left\{1, max\left[0, \frac{(\lambda_2^* - \lambda_1^*)(\omega I^* + \rho\omega I_c^*)S^*}{k_5}\right]\right\},$$

$$u_v^* = min\left\{1, max\left[0, \frac{(\lambda_1^* - \lambda_7^*)(\gamma_3^* S^*)}{k_6}\right]\right\},$$

$$u_r^* = min\left\{1, max\left[0, \frac{-(\lambda_3^* - \lambda_2^*)\eta_2 I_l^*}{k_7}\right]\right\},$$

$$u_t^* = min\left\{1, max\left[0, \frac{(\lambda_3^* - \lambda_5^*)\beta_1 I^* + (\lambda_4^* - \lambda_5^*)\beta_2 I_c^* + (\lambda_5^* - \lambda_6^*)\beta_3 I_h^*}{k_8}\right]\right\}.$$

Proof. Using the transverse condition, the system describes the adjoint variables achieved by differentiating the Hamiltonian as follows:

$$\frac{d\lambda_1}{dt} = -\frac{\partial H}{\partial S}, \quad \frac{d\lambda_2}{dt} = -\frac{\partial H}{\partial I_l}, \quad \frac{d\lambda_3}{dt} = -\frac{\partial H}{\partial I},$$

$$\frac{d\lambda_4}{dt} = -\frac{\partial H}{\partial I_C}, \quad \frac{d\lambda_5}{dt} = -\frac{\partial H}{\partial I_h}, \quad \frac{d\lambda_6}{dt} = -\frac{\partial H}{\partial R},$$

$$\frac{d\lambda_7}{dt} = -\frac{\partial H}{\partial V}.$$

So, the adjoint system can be written as:

$$\begin{aligned} \frac{d\lambda_1}{dt} ={}& 1 + \lambda_1(\omega I + \rho\omega I_c)(1 - u_i) + \lambda_1(\gamma_3 u_v + d_0 + \mu) - \lambda_2(\omega I + \rho\omega I_c)(1 - u_i) - \lambda_7 \gamma_3 u_v, \\ \frac{d\lambda_2}{dt} ={}& -k_1 + \lambda_2(\eta_1(1 - u_r) + d_0 + \mu) - \lambda_3 \eta_1 u_r, \\ \frac{d\lambda_3}{dt} ={}& -k_2 + \omega(1 - u_i)S\lambda_1 - \omega(1 - u_i)S\lambda_2 + \lambda_3(\beta_1 u_t + \gamma_1 + d_0 + \mu) - \lambda_4 \eta_3 \gamma_1 - \lambda_5 \beta_1 u_t - \lambda_6(1 - \eta_3)\gamma_1, \\ \frac{d\lambda_4}{dt} ={}& -k_3 + \Lambda_1 \Lambda_2 \alpha \lambda_1 + \rho\omega(1 - u_i)S\lambda_1 - \rho\omega(1 - u_i)S\lambda_2 + (\beta_2 \eta_2 u_t + d_0 - \Lambda_1 \Lambda_2 \alpha)\lambda_4 - \beta_2 u_t \lambda_5 - \eta_2 \lambda_6, \\ \frac{d\lambda_5}{dt} ={}& -k_4 + (\beta_2 u_t + d_0 + d_2)\lambda_5 - \beta_3 u_t \lambda_6, \end{aligned} \tag{3.6}$$

$$\frac{d\lambda_6}{dt} = d_0\lambda_6,$$

$$\frac{d\lambda_7}{dt} = -\lambda_1\theta + (\theta + d_0)\lambda_7.$$

The optimality conditions are given by:

$$\frac{\partial H}{\partial u_i} = \frac{\partial H}{\partial u_v} = \frac{\partial H}{\partial u_r} = \frac{\partial H}{\partial u_t} = 0. \tag{3.7}$$

Furthermore, we have the following controls

$$u_i = \frac{(\lambda_2 - \lambda_1)(\omega I + \rho\omega I_c)S}{k_5},$$

$$u_v = \frac{(\lambda_1 - \lambda_7)(\gamma_3 S)}{k_6},$$

$$u_r = \frac{-(\lambda_3 - \lambda_2)\eta_2 I_l}{k_7}, \tag{3.8}$$

$$u_t = \frac{(\lambda_3 - \lambda_5)\beta_1 I + (\lambda_4 - \lambda_5)\beta_2 I_c + (\lambda_5 - \lambda_6)\beta_3 I_h}{k_8}.$$

So, the optimal control will be

$$u_i^* = min\left\{1, max\left[0, \frac{(\lambda_2^* - \lambda_1^*)(\omega I^* + \rho\omega I_c^*)S^*}{k_5}\right]\right\},$$

$$u_v^* = min\left\{1, max\left[0, \frac{(\lambda_1^* - \lambda_7^*)(\gamma_3^* S^*)}{k_6}\right]\right\},$$

$$u_r^* = min\left\{1, max\left[0, \frac{-(\lambda_3^* - \lambda_2^*)\eta_2 I_l^*}{k_7}\right]\right\}, \tag{3.9}$$

$$u_t^* = min\left\{1, max\left[0, \frac{(\lambda_3^* - \lambda_5^*)\beta_1 I^* + (\lambda_4^* - \lambda_5^*)\beta_2 I_c^* + (\lambda_5^* - \lambda_6^*)\beta_3 I_h^*}{k_8}\right]\right\}.$$

$\square$

3.2. Numerical simulation of the optimal control problem. In this subsection, we solve the optimal control system (3.1) with the optimal control characterization (3.9) and adjoint system (3.6) numerically with the finite difference scheme. First, we discretize the optimal control system (3.1) to get the following equations:

$$(S)^{m+1} = (S)^m + \tau\Lambda_1\Lambda_2\left(1 - \alpha(I_c)^m\right) - \tau\left((\omega(I)_j^m + \rho\omega(I_c)^m)(1 - (u_i)^m)(S)^{m+1}\right)$$
$$- \tau\left(\gamma_3(u_v)^m + d + \mu\right)(S)^{m+1} + \tau\theta(V)^m, \tag{3.10}$$

$$(I_l)^{m+1} = (I_l)^m + \tau\left(\omega(I)^m + \rho\omega(I_c)_j^m\right)(1 - (u_i)^m)(S)^m - \tau\left(\eta_1(1 - (u_r)^m) + d + \mu\right)(I_l)^{m+1}, \tag{3.11}$$

$$(I)^{m+1} = (I)^m - \tau\left(\beta_1(u_t)^m + \gamma_1 + d + \mu\right)(I)^{m+1} + \tau\eta_1(u_r)^m(I_l)^m, \tag{3.12}$$

$$(I_c)^{m+1} = (I_c)^m + \tau\eta_3\gamma_1(I)^m - \tau\left(\beta_2\eta_2(u_t)^m + d + d_1 - \Lambda_1\Lambda_2\alpha\right)(I_c)^{m+1}, \tag{3.13}$$

$$(I_h)^{m+1} = (I_h)^m + \tau\beta_2(u_t)^m(I_c)_j^m - \tau\left(\beta_3(u_t)^m + d + d_2\right)(I_h)^{m+1} + \tau(u_t)^m\beta_1(I)^m, \tag{3.14}$$

$$(R)^{m+1} = (R)^m + +\tau\eta_2(I_c)_j^m + \tau\left(1 - \eta_3\right)\gamma_1(I)_j^m + \tau\beta_3(u_t)^m(I_h)^m - \tau d(R)^{m+1}, \tag{3.15}$$

$$(V)^{m+1} = (V)^m + \tau\Lambda_1\left(1 - \Lambda_2\right) + \tau\gamma_3(u_v)^m(S)^m - \tau\left(\theta + d\right)(V)^{m+1}. \tag{3.16}$$

C M
D E

Also, discretize the optimal control characterization equations as follows:

$$(u_i)^m = min\left\{1, max\left[0, \frac{((\lambda_2)^m - (\lambda_1)^m)(\omega(I)^m + \rho\omega(I_c)^m)(S)^m}{k_5}\right]\right\}, \tag{3.17}$$

$$(u_v)^m = min\left\{1, max\left[0, \frac{((\lambda_1)^m - (\lambda_7)^m)(\gamma_3(S)^m)}{k_6}\right]\right\}, \tag{3.18}$$

$$(u_r)^m = min\left\{1, max\left[0, \frac{-((\lambda_3)^m - (\lambda_2)^m)\eta_2(I_l)^m}{k_7}\right]\right\}, \tag{3.19}$$

$$(u_t)^m = min\left\{1, max\left[0, \frac{((\lambda_3)^m - (\lambda_5)^m)\beta_1 I^* + ((\lambda_4)^m - (\lambda_5)^m)\beta_2(I_c)^m + ((\lambda_5)^m - (\lambda_6)^m)\beta_3(I_h)^m}{k_8}\right]\right\}. \tag{3.20}$$

Also, discretize the adjoint equations as follow:

$$\begin{aligned}(\lambda_1)^{m+1} &= (\lambda_1)^m + 1 + (\lambda_1)^{m+1}(\omega(I)^m + \rho\omega(I_c)^m)(1 - (u_i)^m) \\ &+ (\lambda_1)^{m+1}(\gamma_3(u_v)^m + d + \mu) - (\lambda_2)^{m+1}(\omega(I)^m + \rho\omega(I_c)^m)(1 - (u_i)^m) - (\lambda_7)^{m+1}\gamma_3(u_v)^m,\end{aligned} \tag{3.21}$$

$$(\lambda_2)^{m+1} = (\lambda_2)^m - k_1 + (\lambda_2)^m(\eta_1(1 - (u_r)^m) + d + \mu) - (\lambda_3)^m\eta_1(u_r)^m, \tag{3.22}$$

$$\begin{aligned}(\lambda_3)^{m+1} &= (\lambda_3)^m - k_2 + \omega(1 - (u_i)^m)(S)^m(\lambda_1)^m - \omega(1 - (u_i)^m)(S)^m(\lambda_2)^m \\ &- (\lambda_4)^m\eta_3\gamma_1 + (\lambda_3)^m(\beta_1(u_t)^m + \gamma_1 + d + \mu) - (\lambda_5)^m\beta_1(u_t)^m - (\lambda_6)^m(1 - \eta_3)\gamma_1,\end{aligned} \tag{3.23}$$

$$\begin{aligned}(\lambda_4)^{m+1} &= (\lambda_4)^m - k_3 + \Lambda_1\Lambda_2\alpha(\lambda_1)^m + \rho\omega(1 - (u_i)^m)S(\lambda_1)^m \\ &- \rho\omega(1 - (u_i)^m)(S)^m(\lambda_2)^m + (\beta_2\eta_2(u_t)^m + d - \Lambda_1\Lambda_2\alpha)(\lambda_4)^m - \beta_2(u_t)^m(\lambda_5)^m - \eta_2(\lambda_6)^m,\end{aligned} \tag{3.24}$$

$$(\lambda_5)^{m+1} = (\lambda_5)^m - k_4 + (\beta_2(u_t)^m + d + d_2)(\lambda_5)^m - \beta_3(u_t)^m(\lambda_6)^m, \tag{3.25}$$

$$(\lambda_6)^{m+1} = (\lambda_6)^m + d(\lambda_6)^m, \tag{3.26}$$

$$(\lambda_7)^{m+1} = (\lambda_7)^m - (\lambda_1)^m\theta + (\theta + d)(\lambda_7)^m. \tag{3.27}$$

Taking into account $\lambda_i(t_f) = 0, i = 1, 2, 3, ..., 7$ and t_f represent the final time and $k_i = 1$ with $i = 1, 2, ..., 7$. We solve the optimal state system (3.1) and the adjoint state system (3.6) by forward and backward finite difference schemes, respectively. Using Mathematica 12 package, the optimal control problem is solved with an iterative scheme via an initial guess for the control variables. The new values of control variables are computed and then we repeat the previous steps with the new control variable to get new values for state and adjoint variables until we reach the optimal state.

The sub-graphs in Figure 2 show the dynamics of susceptible, infected individuals in four categories, recovered and vaccinated individuals. It can be observed from the results that four controls considered in this simulation are very effective in reducing the severity of infection among people, as shown in Figures 2(b, c, d, e). Also, Figure 2 shows the numerical solution of the HBV system before and after applying four types of optimal control together. We find that all infection categories decrease over time, as shown in blue. However, after applying optimal control to this system, we notice in Figure 2(b) in red color that the numbers in the I_l category decrease more clearly. This category is considered the most dangerous type of infection, as it does not show clear symptoms and can transmit the disease to other people, increasing the infection rate. We also observe a reduction in the numbers in Figures 2(c, d, e), where the number of patients in these categories also decreases significantly. Over time, the number of people receiving vaccinations decreases, as shown in Figure 2(g), due to the reduction in the number of infected individuals. Additionally, we notice an increase in the number of recovered patients over time, as illustrated in Figure 2(f). In Figure 3, we apply two types of optimal control only: isolation and vaccination. We observe that the number of infections decreases in the four Infection categories as shown in Figures 3(b, c, d, e), but to a lesser extent than the results obtained by applying all four controls together. As in Figure 3(b), the number of individuals in the latent category (is the most dangerous) decreases, but not as significantly as in Figure 2(b). Therefore, we urge governments

to implement all four controls to reduce the number of infections, increase the number of recoveries, and ultimately eradicate HBV over time.

4. SPATIO-TEMPORAL STUDY

4.1. **spatio-temporal mathematical model of HBV.**
In this subsection, we present a numerical simulation of the spatio-temporal model of the hepatitis B virus, which can be defined as follows:

$$
\begin{aligned}
\frac{\partial S}{\partial t} &= M_1 \frac{\partial^2 S}{\partial x^2} + \Lambda_1 \Lambda_2 (1 - \alpha I_c(t)) + \theta V(t) - (\omega I(t) + \rho \omega I_c(t) + \gamma_3 + d_0 + \mu)S(t), \\
\frac{\partial I_l}{\partial t} &= M_2 \frac{\partial^2 I_l}{\partial x^2} + (\omega I(t) + \rho \omega I_c(t))S(t) - (\eta_1 + d_0 + \mu)I_l(t), \\
\frac{\partial I}{\partial t} &= M_3 \frac{\partial^2 I}{\partial x^2} - (\beta_1 + \gamma_1 + d_0 + \mu)I(t) + \eta_1 I_l(t), \\
\frac{\partial I_c}{\partial t} &= M_4 \frac{\partial^2 I_c}{\partial x^2} + \eta_3 \gamma_1 I(t) - (\beta_2 \eta_2 + d_0 + d_1 - \Lambda_1 \Lambda_2 \alpha)I_c(t), \\
\frac{\partial I_h}{\partial t} &= M_5 \frac{\partial^2 I_h}{\partial x^2} + \beta_2 I_c(t) + \beta_1 I(t) - (\beta_3 + d_0 + d_2)I_h(t), \\
\frac{\partial R}{\partial t} &= M_6 \frac{\partial^2 R}{\partial x^2} + \eta_2 I_c(t) + (1 - \eta_3)\gamma_1 I(t) + \beta_3 I_h(t) - d_0 R(t), \\
\frac{\partial V}{\partial t} &= M_7 \frac{\partial^2 V}{\partial x^2} + \Lambda_1 (1 - \Lambda_2) + \gamma_3 S(t) - (\theta + d_0)V(t),
\end{aligned}
\tag{4.1}
$$

with initial conditions (4.2) and homogeneous Neumann boundary conditions (4.3):

$$
\begin{aligned}
&S(0,x) = 2S_0 x(1-x), I_l(0,x) = 2I_{l_0} x(1-x), \\
&I(0,x) = 2I_0 x(1-x), I_c(0,x) = 2I_{c_0} x(1-x), \\
&I_c(0,x) = 2I_{h_0} x(1-x), R(0,x) = 2R_0 x(1-x), \\
&V(0,x) = 2V_0 x(1-x).
\end{aligned}
\tag{4.2}
$$

$$
\begin{aligned}
&\frac{\partial S(t,0)}{\partial x} = \frac{\partial S(t,1)}{\partial x} = 0, \frac{\partial I_l(t,0)}{\partial x} = \frac{\partial I_l(t,1)}{\partial x} = 0, \\
&\frac{\partial I(t,0)}{\partial x} = \frac{\partial I(t,1)}{\partial x} = 0, \frac{\partial I_c(t,0)}{\partial x} = \frac{\partial I_c(t,1)}{\partial x} = 0, \\
&\frac{\partial I_h(t,0)}{\partial x} = \frac{\partial I_h(t,1)}{\partial x} = 0, \frac{\partial R(t,0)}{\partial x} = \frac{\partial R(t,1)}{\partial x} = 0, \\
&\frac{\partial V(t,0)}{\partial x} = \frac{\partial V(t,1)}{\partial x} = 0.
\end{aligned}
\tag{4.3}
$$

This model consists of seven partial differential equations that represent the prevalence of B virus disease, where x and t represent space and time, respectively. The initial conditions are set in such a manner that the proportion of infected people reaches its maximum value in a specific area of space and then decreases slightly as one moves away from this area. The boundary conditions are used in the form of homogeneous Neumann conditions for the reason that when an epidemic spreads in a certain area, this condition guarantees that people will not enter or leave this area and this is called a complete closure. The model can then be used to detect changes in infectious diseases and their regional variations over time.

4.2. **Numerical simulation and graphical results.**
In this subsection, we introduce a numerical study of the spatio-temporal model of HBV (4.1) as in the following steps:

Step1: Beginning with dividing the domain of $x \in [0,1]$ and $t \in [0,50]$ into $10^2 \times 50$ cubes with step size $h = 0.1$ and
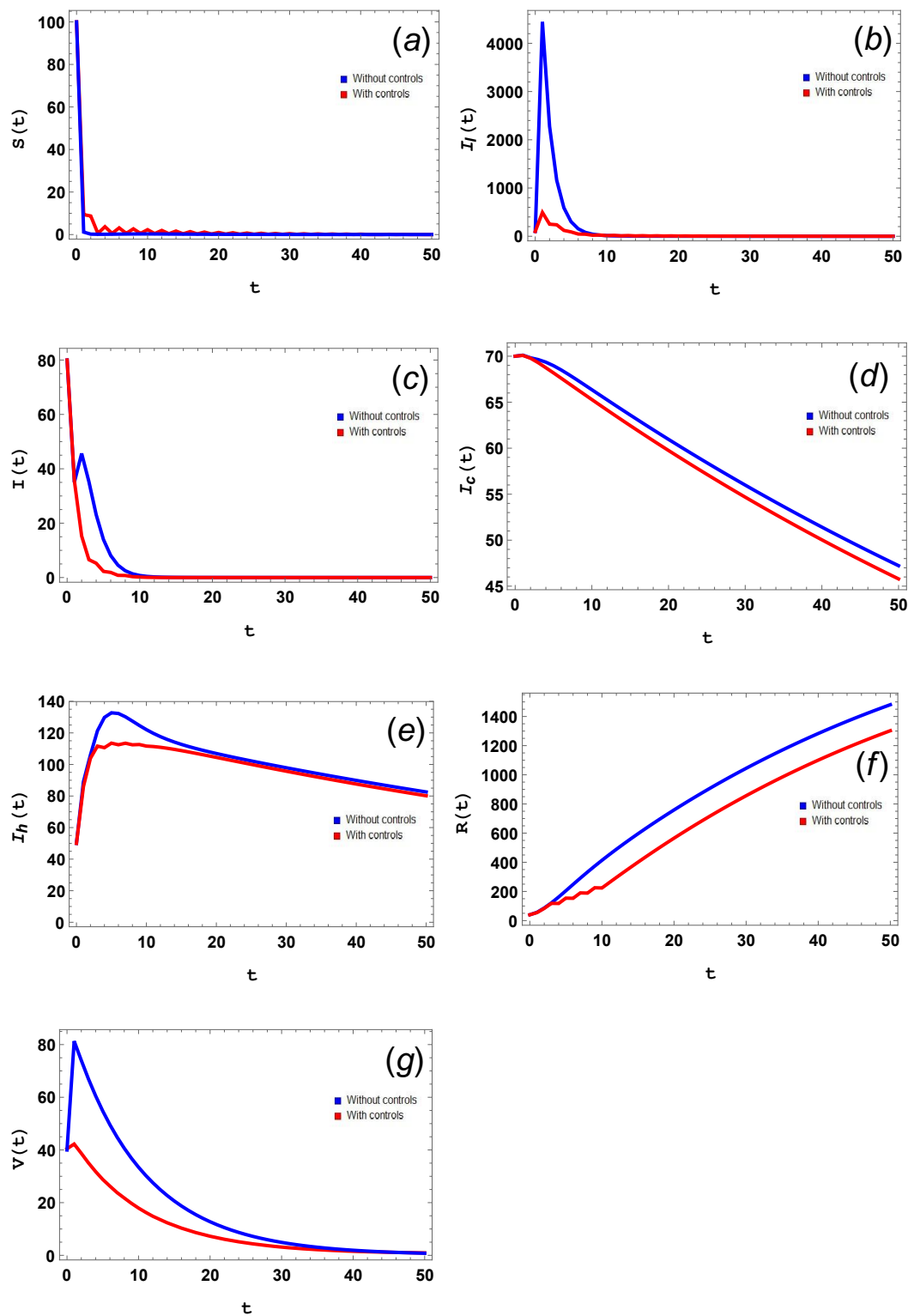
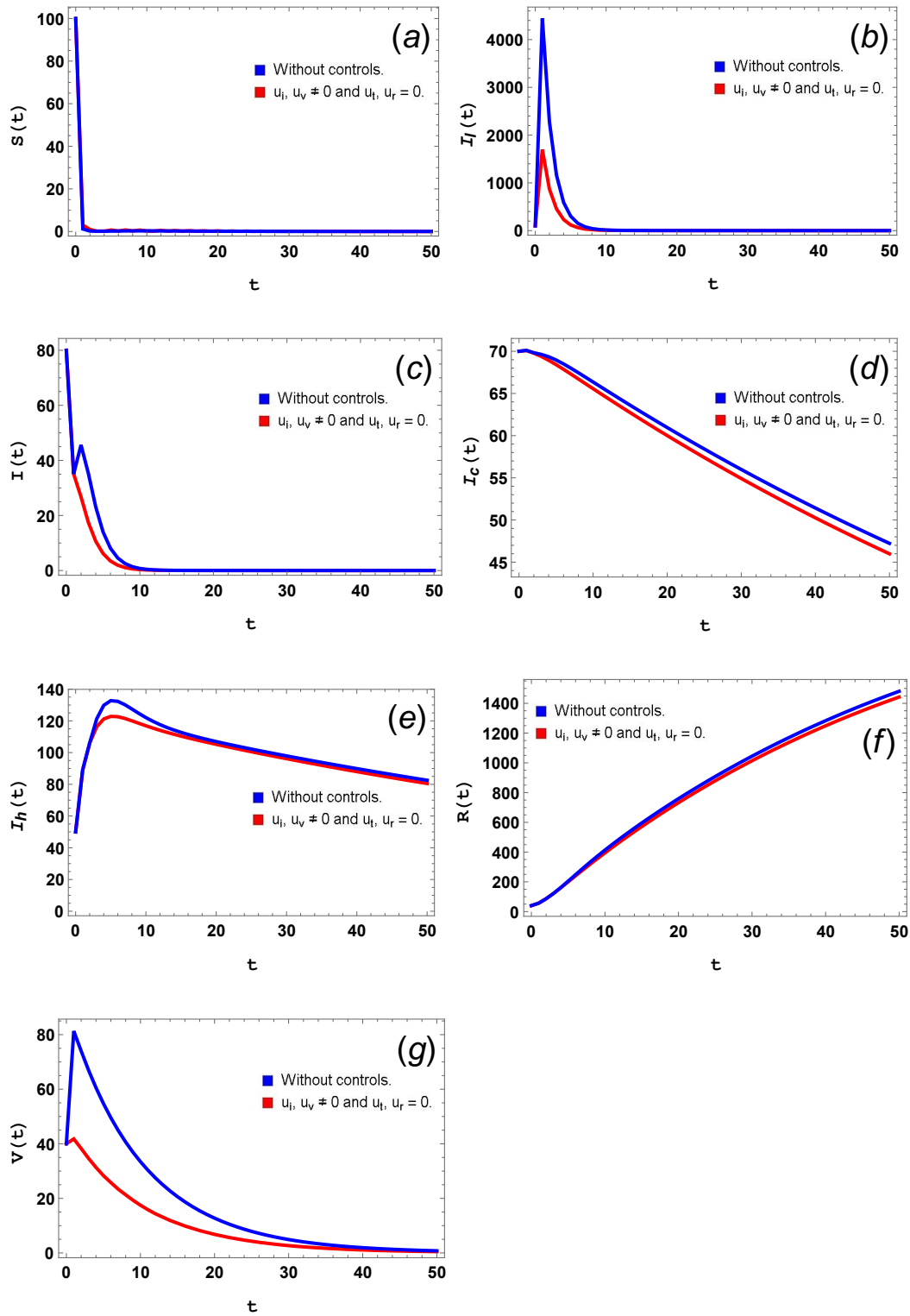FIGURE 2. Comparison of the temporal model results with and without controls.

FIGURE 3. Comparison of the temporal model results with two types of controls and without controls.

$\Delta t = 1$, we apply the finite difference scheme as follows:

$$\frac{\partial S}{\partial t} = \frac{(S)_j^{m+1} - (S)_j^m}{\Delta t},$$
$$\frac{\partial^2 S}{\partial x^2} = \frac{n(S)_{j+1}^{m+1} - 2(S)_j^{m+1} + (S)_{j-1}^{m+1}}{\Delta x^2}.$$

(4.4)

Step 2: By discretizing the system (4.1) and its boundary conditions (4.3), we get the following system of equations:

$$(S)_j^{m+1} = (S)_j^m + \frac{\Delta t M_1}{(\Delta x)^2}\Big((S)_{j+1}^{m+1} - 2(S)_j^{m+1} + (S)_{j-1}^{m+1}\Big) + \Delta t\theta(V)_j^m$$
$$+ \Delta t\Lambda_1\Lambda_2\Big(1 - \alpha(I_c)_j^m + 1\Big) - \Delta t\Big(\omega(I)_j^m + \rho\omega(I_c)_j^m + \gamma_3 + d_0 + \mu\Big)(S)_j^{m+1},$$

(4.5)

$$(I_l)_j^{m+1} = (I_l)_j^m + \frac{\Delta t M_2}{(\Delta x)^2}\Big((I_l)_{j+1}^{m+1} - 2(I_l)_j^{m+1} + (I_l)_{j-1}^{m+1}\Big) + \Delta t\Big(\omega(I)_j^m$$
$$+ \rho\omega(I_c)_j^m\Big)(S)_j^m - \Delta t\Big(\eta_1 + d_0 + \mu\Big)(I_l)_j^{m+1},$$

(4.6)

$$(I)_j^{m+1} = (I)_j^m + \frac{\Delta t M_3}{(\Delta x)^2}\Big((I)_{j+1}^{m+1} - 2(I)_j^{m+1} + (I)_{j-1}^{m+1}\Big) - \Delta t\Big(\beta_1 + \gamma_1 + d_0 + \mu\Big)(I)_j^{m+1} + \Delta t\eta_1(I_l)_j^m,$$

(4.7)

$$(I_c)_j^{m+1} = (I_c)_j^m + \frac{\Delta t M_4}{(\Delta x)^2}\Big((I_c)_{j+1}^{m+1} - 2(I_c)_j^{m+1} + (I_c)_{j-1}^{m+1}\Big) + \Delta t\eta_3\gamma_1(I)_j^m$$
$$- \Delta t\Big(\beta_2\eta_2 + d_0 + d_1 - \Lambda_1\Lambda_2\alpha\Big)(I_c)_j^{m+1},$$

(4.8)

$$(I_h)_j^{m+1} = (I_h)_j^m + \frac{\Delta t M_5}{(\Delta x)^2}\Big((I_h)_{j+1}^{m+1} - 2(I_h)_j^{m+1} + (I_h)_{j-1}^{m+1}\Big) + \Delta t\beta_2(I_c)_j^m$$
$$+ \Delta t\beta_1(I)_j^m - \Delta t\Big(\beta_3 + d_0 + d_2\Big)(I_h)_j^{m+1},$$

(4.9)

$$(R)_j^{m+1} = (R)_j^m + \frac{\Delta t M_6}{(\Delta x)^2}\Big((R)_{j+1}^{m+1} - 2(R)_j^{m+1} + (R)_{j-1}^{m+1}\Big) + \Delta t\eta_2(I_c)_j^m$$
$$+ \Delta t\Big(1 - \eta_3\Big)\gamma_1(I)_j^m + \Delta t\beta_3(I_h)_j^m - \Delta t d_0(R)_j^{m+1},$$

(4.10)

$$(V)_j^{m+1} = (V)_j^m + \frac{\Delta t M_6}{(\Delta x)^2}\Big((V)_{j+1}^{m+1} - 2(V)_j^{m+1} + (V)_{j-1}^{m+1}\Big)$$
$$+ \Delta t\Lambda_1\Big(1 - \Lambda_2\Big) + \Delta t\gamma_3(S)_j^m - \Delta t\Big(\theta + d_0\Big)(V)_j^{m+1},$$

(4.11)

Step 3: Solve the algebraic system (4.5)-(4.11).
Step 4: Update the values of the variables at each grid point based on the solution obtained.
Step 5: Repeat iteratively,
where the diffusion coefficients are $M_i = 0.01, i = 1, 2, 3, ..., 7$ and the graphical simulation of the numerical solution as shown in Figure 4. It is very clear that staying away from the place of infection reduces the spread of the virus. This displays the importance of isolation to stop the spread of the disease.

4.3. **Truncation Error.** In this subsection, we look at the proposed scheme's consistency. By using Taylor expansion with the system (4.1), we get:

$$\Psi_S = \frac{(S)_j^{m+1} - (S)_j^m}{\Delta t} - \frac{M_1}{(\Delta x)^2}\Big((S)_{j+1}^{m+1} - 2(S)_j^{m+1} + (S)_{j-1}^{m+1}\Big) - \theta(V)_j^m$$
$$- \Lambda_1\Lambda_2\Big(1 - \alpha(I_c)_j^m + 1\Big) + \Big(\omega(I)_j^m - \rho\omega(I_c)_j^m + \gamma_3 + d_0 + \mu\Big)(S)_j^{m+1},$$

(4.12)
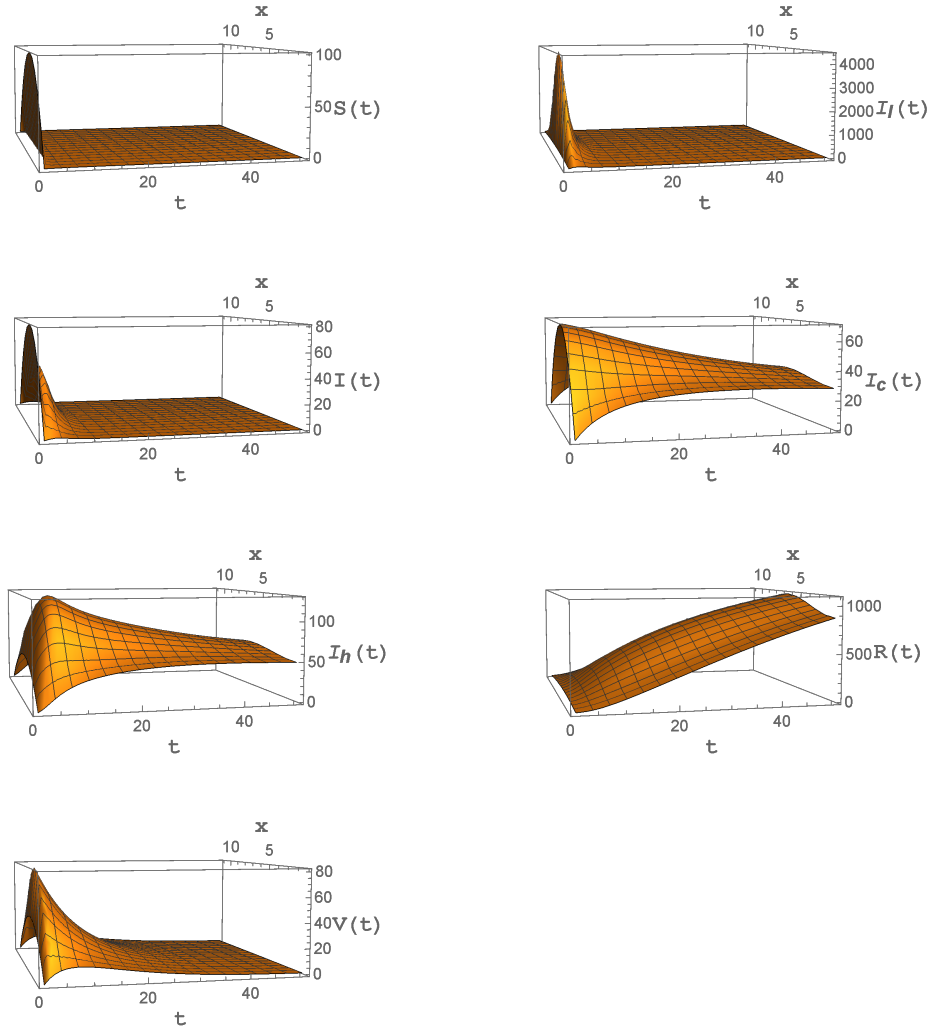
FIGURE 4. 3D graphical numerical results of the spatio-temporal HBV model.

$$\Psi_S = \left(\frac{\partial S}{\partial t} + \frac{\Delta t}{2!} \frac{\partial^2 S}{\partial t^2} + \frac{\Delta t^2}{3!} \frac{\partial^2 S}{\partial t^2} + ... \right) - \Lambda_1 \Lambda_2 \Big(1 - \alpha(I_c)_j^m + 1 \Big) - \theta(V)_j^m$$

$$- \frac{M_1}{(\Delta x)^2} \left(\Delta x^2 \Big(\frac{\partial^2 S}{\partial x^2} + 2 \frac{\Delta x^2}{4!} \frac{\partial^4 S}{\partial x^4} + ... \Big) \right) + \Big(\omega(I)_j^m - \rho\omega(I_c)_j^m + \gamma_3 + d_0 + \mu \Big)$$

$$* \left((S)_j{}^m + \Delta t \frac{\partial S}{\partial t} + \frac{\Delta t^2}{2!} \frac{\partial^2 S}{\partial t^2} + \frac{\tau^3}{3!} \frac{\partial^2 S}{\partial t^2} + ... \right), \tag{4.13}$$

$$\Psi_S = \frac{\partial S}{\partial t} - \frac{M_1(\Delta x)^2}{(\Delta x)^2} \frac{\partial^2 S}{\partial x^2} + (S)_j{}^m \Big(\omega(I)_j^m - \rho\omega(I_c)_j^m + \gamma_3 + d_0 + \mu \Big)$$

$$- \Lambda_1 \Lambda_2 \Big(1 - \alpha(I_c)_j^m + 1 \Big) - \theta(V)_j^m - \frac{2M_1 \Delta x^4}{(4!\Delta x)^2} \frac{\partial^4 S}{\partial x^4} \tag{4.14}$$

$$+ \Delta t \left(\left(\omega(I)_j^m - \rho\omega(I_c)_j^m + \gamma_3 + d_0 + \mu \right) \left(\frac{\partial S}{\partial t} + ... \right) \right),$$

$$\Psi_S = -\frac{2M_1\Delta x^2}{4!} \frac{\partial^4 S}{\partial x^4} + \Delta t \left(\left(\omega(I)_j^m - \rho\omega(I_c)_j^m + \gamma_3 + d_0 + \mu \right) \left(\frac{\partial S}{\partial t} + ... \right) \right). \tag{4.15}$$

So, $\Psi_S \to 0$ as $\Delta x \to 0$ and $\Delta t \to 0$.

Also, we can obtain the relations for I_l, I, I_c, I_h, R, and V as follows:

$$\Psi_{I_l} = -\frac{2M_2\Delta x^2}{4!} \frac{\partial^4 I_l}{\partial x^4} + \Delta t \left(\left(\eta_1 + d_o + \mu \right) \left(\frac{\partial I_l}{\partial t} + ... \right) \right),$$

$$\Psi_I = -\frac{2M_3\Delta x^2}{4!} \frac{\partial^4 I}{\partial x^4} + \Delta t \left(\left(\beta_1 + \gamma_1 + d_0 + \mu \right) \left(\frac{\partial I}{\partial t} + ... \right) \right),$$

$$\Psi_{I_c} = -\frac{2M_3\Delta x^2}{4!} \frac{\partial^4 I_c}{\partial x^4} + \Delta t \left(\left(\beta_2\eta_2 + d_0 + d_1 - \Lambda_1\Lambda_2\alpha \right) \left(\frac{\partial I_c}{\partial t} + ... \right) \right),$$

$$\Psi_{I_h} = -\frac{2M_3\Delta x^2}{4!} \frac{\partial^4 I_h}{\partial x^4} + \Delta t \left(\left(\beta_3 + d_0 + d_2 \right) \left(\frac{\partial I_h}{\partial t} + ... \right) \right), \tag{4.16}$$

$$\Psi_R = -\frac{2M_3\Delta x^2}{4!} \frac{\partial^4 R}{\partial x^4} + \Delta t \left(\left(d_0 \right) \left(\frac{\partial R}{\partial t} + ... \right) \right),$$

$$\Psi_V = -\frac{2M_3\Delta x^2}{4!} \frac{\partial^4 V}{\partial x^4} + \Delta t \left(\left(d_0 + \theta \right) \left(\frac{\partial V}{\partial t} + ... \right) \right),$$

then from the previous Equations (4.15) and (4.16), we find that $\Psi_S, \Psi_{I_l}, \Psi_I, \Psi_{I_c}, \Psi_{I_h}, \Psi_R, \Psi_V \to 0$ as $\Delta x \to 0$ and $\Delta t \to 0$. Hence, this scheme has an accuracy of $O(\Delta t, \Delta x^2)$.

4.4. **Von-Neumann stability for numerical scheme.** This subsection proves that the proposed numerical scheme is stable at Von Neumann. First, we define:

$$(S)_j^m = \phi_s^m e^{i\xi_s j\Delta x}, \quad (S)_j^{m+1} = \phi_s^{m+1} e^{i\xi_s j\Delta x},$$

$$(S)_{j+1}^{m+1} = \phi_s^{m+1} e^{i\xi_s (j+1)\Delta x}. \tag{4.17}$$

Substituting from (4.17) into (4.5) and nonlinear terms, we get

$$(S)_j^{m+1} \left(1 + 2y_1 + \Delta t \left(\omega(I)_j^m + \rho\omega(I_c)_j^m + \gamma_3 + d_0 + \mu \right) \right)$$

$$- y_1 \left((S)_{j+1}^{m+1} + (S)_{j-1}^{m+1} \right) = (S)_j^m + \Delta t \Lambda_1\Lambda_2 \left(1 - \alpha(I_c)_j^m + 1 \right) + \Delta t\theta(V)_j^m. \tag{4.18}$$

Now, we define the amplification factor as $E_s = \dfrac{(S)_j^{m+1}}{(S)_j^m}$ and substitute in (4.18), we get

$$E_s \left(1 + 2y_1 + \Delta t \left(\gamma_3 + d_0 + \mu \right) \right) + \Delta t\acute{\nu}_1 \right) - y_1 \left(E_s e^{-i\xi_s\Delta x} + E_s e^{i\xi_s\Delta x} \right) = 1, \tag{4.19}$$

where y_1 is mesh ratio which equals to $\frac{\Delta t M_1}{(\Delta x)^2}$ and $\acute{\nu}_1 = \omega(I)_j^m + \rho\omega(I_c)_j^m$ then, we get

$$E_s \left(1 + \Delta t \left(\acute{\nu}_1 + \gamma_3 + d_0 + \mu \right) + 4y_1 \sin^2(\frac{\xi_s\Delta x}{2}) \right) = 1. \tag{4.20}$$

Then

$$E_S = \frac{1}{1 + \Delta t\left(\dot{\nu}_1 + \gamma_3 + d_0 + \mu\right) + 4y_1 \sin^2(\frac{\xi_S \Delta x}{2})}, \tag{4.21}$$

which implies that $E_S \leq 1$ is the necessary and sufficient condition for the error to remain bounded and maintain numerical stability.

Similarly, by following the same previous steps, we obtain

$$E_L = \left| \frac{1}{1 + \Delta t\left(\eta_1 + d_0 + \mu\right) + 4y_1 \sin^2(\frac{\xi_l \Delta x}{2})} \right| \leq 1,$$

$$E_I = \left| \frac{1}{1 + \Delta t\left(\beta_1 + \gamma_1 + d_0 + \mu\right) + 4y_1 \sin^2(\frac{\xi_I \Delta x}{2})} \right| \leq 1,$$

$$E_C = \left| \frac{1}{1 + \Delta t\left(\beta_2 \eta_2 + d_0 + d_1 - \Lambda_1 \Lambda_2 \alpha\right) + 4y_1 \sin^2(\frac{\xi_C \Delta x}{2})} \right| \leq 1,$$

$$E_H = \left| \frac{1}{1 + \Delta t\left(\beta_3 + d_0 + d_2\right) + 4y_1 \sin^2(\frac{\xi_H \Delta x}{2})} \right| \leq 1, \tag{4.22}$$

$$E_R = \left| \frac{1}{1 + \Delta t\left(d_0\right) + 4y_1 \sin^2(\frac{\xi_R \Delta x}{2})} \right| \leq 1,$$

$$E_V = \left| \frac{1}{1 + \Delta t\left(\theta + d_0\right) + 4y_1 \sin^2(\frac{\xi_V \Delta x}{2})} \right| \leq 1.$$

All inequalities in (4.21) and (4.22) show that the proposed scheme is Von-Neumann stable.

5. Conclusion

We formulated a mathematical model for HBV infection with optimal control theory. The optimal control system was edited using four different types of controls. The optimality system has been solved and the results were great for infection reduction. The spatio-temporal model was constructed and numerically solved. In addition, the study was conducted for the stability and consistency of the numerical scheme. Numerical results of the spatio-temporal model showed the importance of quarantine to stop the spread of the disease.

References

[1] S. Ahmad, M. Rahman, and M. Arfan, *On the analysis of semi-analytical solutions of hepatitis B epidemic model under the Caputo-Fabrizio operator*, Chaos, Solitons and Fractals, *146* (2021), 110892.

[2] N. Akbari and R. Asheghi, *Optimal control of an HIV infection model with logistic growth, celluar and homural immune response, cure rate and cell-to-cell spread*, Boundary Value Problems, (2022), 1–12.

[3] H. Alrabaiah, M. Safi, M. DarAssi, B. Al-Hdaibat, S. Ullah, M. Khan, and S. Shah, *Optimal control analysis of hepatitis B virus with treatment and vaccination*, Results in Physics, *19* (2020), 103599.

[4] M. Bachraoui, M. Ichou, K. Hattaf, and N. Yousfi, *Spatiotemporal dynamics of a fractional model for hepatitis B virus infection with cellular immunity*, Mathematical Modelling of Natural Phenomena, *16*(49) (2020).

[5] A. Din, Y. Li, and M. Shah, *The complex dynamics of hepatitis B infected individuals with optimal control*, J. Syst. Sci. Complex, *34*(4) (2020), 1301–1323.

[6] I. Fitria and A. Syafi'i, *An epidemic cholera model with control treatment and intervention*, Journal of Physics, *1218* (2019), 012046.

[7] H. Gaff, *Optimal control applied to vaccination and treatment strategies for various epidemiological models*, Mathematical Biosciences and Engineering, *6* (2009), 469–492.

[8] T. Khan, S. Ahmad, and G. Zaman, *Modeling and qualitative analysis of a hepatitis B epidemic model*, Chaos, Solitons and Fractals, *29* (2019), 103139.

[9] A. Koura, K. Raslan, K. Ali, and M. Shaalan, *Numerical analysis of a spatio-temporal bi modal coronavirus disease pandemic*, Applied Mathematics and Information Sciences, *16*(5) (2022), 729–737.

[10] K. Manna and K. Hattaf, *Spatiotemporal Dynamics of a Generalized HBV Infection Model with Capsids and Adaptive Immunity*, Int. J. Appl. Comput. Math, *65* (2019), 1–29.

[11] R. Neilan, E. Schaefer, H. Gaff, K. R. Fister, and S. Lenhart, *Modeling Optimal Intervention Strategies for Cholera*, Bulletin of Mathematical Biology, *72* (2010) , 2004–2018.

[12] A. Raza, A. Ahmadian, M. Rafiq, S. Salahshour, M. Naveed, M. Ferrara, and A. Soori, *Modeling the effect of delay strategy on transmission dynamics of HIV/AIDS disease*, Advances in Difference Equations, *663* (2020), 1–13.

[13] S. Sahaa and G. Samantaa, *Modelling and optimal control of HIV/AIDS prevention through PrEP and limited treatment*, Physica A, *516* (2019), 280–307.

[14] O. Sharomi and T. Malik, *Optimal control in epidemiology*, Ann. Oper. Res., *251* (2017), 55–71.

[15] G. Zaman, Y. Kang, and I. Jung, *Optimal treatment of an SIR epidemic model with time delay*, BioSystems, *98* (2009), 43–50.

[16] M. Zorom, P. Zongo, B. Barbier, and B. Some, *Optimal Control of a spatio-temporal Model for Malaria: Synergy Treatment and Prevention*, Journal of Applied Mathematics, *854723* (2012), 1–20.

[17] L. Zou, W. Zhang, and S. Ruan, *Modeling the transmission dynamics and control of hepatitis B virus in China*, Journal of Theoretical Biology, *262* (2010), 330–338.